BJPS

Brazilian Journal of Pharmaceutical Sciences

http://dx.doi.org/10.1590/s2175-97902024e23797

Article

In-silico Studies of Epoxy-Thioxanthone Derivatives as Potential Tyrosine Kinase Inhibitor Using Molecular Docking, Molecular Dynamics Simulations, MM-PBSA and ADMET

Faris Hermawan[1*], Jumina Jumina[2], Harno Dwi Pranowo[3], Teni Ernawati[1], Yehezkiel Steven Kurniawan[2], Adi Tiara Zikri[4]

[1]Research Center for Pharmaceutical Ingredient and Traditional Medicine, National Research and Innovation Agency (BRIN), Indonesia, [2]Department of Chemistry, Faculty of Mathematics and Natural Sciences, Universitas Gadjah Mada, Indonesia, [3]Austrian-Indonesian Centre (AIC) for Computational Chemistry, Department of Chemistry, Faculty of Mathematics and Natural Sciences, Universitas Gadjah Mada, Indonesia, [4]Department of Materials Science and Engineering, Chonnam National University, Republic of Korea

Protein tyrosine kinases play a role in the cell signaling pathways involving cell growth, differentiation, apoptosis, and metabolism of cancer cells. Because of that, the molecular docking, molecular dynamics, MM-PBSA, and prediction ADMET properties were conducted to evaluate the inhibition activity of epoxy-thioxanthones against platelet-derived growth factors receptor (PDGFR) and epidermal growth factor receptor (EGFR) proteins. A series of ten thioxanthone compounds bearing hydroxy, epoxy, chloro, and bromo substituents have been designed and evaluated. The docking results showed that the epoxy-thioxanthones (**A-J**) have binding energy from -7.12 to -9.81 and -7.24 to -8.06 kcal/mol against those proteins, respectively. Compared with the native ligands, all epoxy-thioxanthones gave stronger binding energy (-7.24 to -8.06 kcal/mol) with the active site of EGFR than the erlotinib (-7.05 kcal/mol), which is remarkable. This result is also in line with the molecular dynamics results. The calculation of binding energy MM-PBSA that compounds **D**, **E**, **I**, and **J** had comparable EGFR protein stability to erlotinib. The binding energy of those compounds (-19.29 to -29.35 kcal/mol) had lower than erlotinib (-8.25 kcal/mol). Furthermore, in physicochemical properties prediction, those compounds fulfill Lipinski's rule parameters and the minimum standard parameters in ADMET properties.

Keywords: Molecular Docking. Molecular Dynamic. ADMET properties. Epoxy thioxanthone. PDGFR. EGFR.

INTRODUCTION

Cancer is a deadly disease characterized by rapid, uncontrolled, and pathological proliferation of abnormal cells (Karabacak *et al*., 2015). Globally, cancer is the second most serious disease that causes 10 million deaths in 2020 (Sung *et al*., 2021). The condition is worsened by low selectivity, resistance, and side effects of chemotherapy agents (Wahyuningsih, Suma, Astuti, 2019). It was reported that some pathological diseases, such as cancer, atherosclerosis, and psoriasis, are caused by uncontrolled signaling from intracellular tyrosine kinase receptors (Shah *et al*., 2018). Therefore, protein tyrosine kinases (PTK) play a key role in cell signaling pathways involving cell growth, differentiation, apoptosis, and metabolism. Because of that, it is indispensable to develop a better anticancer agent to inhibit the PTK; thus,

***Correspondence:** F Hermawan. Email: fari025@brin.go.id. ORCID: https://orcid.org/0009-0006-6923-4050

the cell growth, apoptosis, and angiogenesis of cancer cells can be suppressed.

Protein tyrosine kinases such as platelet-derived growth factors receptor (PDGFR) and epidermal growth factor receptor (EGFR) have a critical role in the metabolism of cancer cells. PDGFR protein is essential in cancer cell proliferation, survival, migration, and differentiation (Kanaan, Strange, 2017). The inhibitors of PDGFR could block those roles. The inhibitor that is selective for the PDGFR protein is imatinib (Coban, Degim, 2020). Imatinib inhibits the growth of ovarian cancer cells at clinically relevant concentrations (IC_{50} < 1 μM) by specifically inhibiting the protein PDGFR (Matei, Chang, Jeng, 2004). Imatinib also inhibits medulloblastoma cell migration and invasion by suppressing PDGFR activation and EGFR transactivation (Abouantoun, MacDonald, 2009). Imatinib, which has been used for over 20 years, is widely regarded as the safest tyrosine kinase inhibitor (TKI), with no long-term irreversible side effects reported. The 2G and 3GTKIs have distinct risk profiles with more severe consequences. The most serious and not always completely reversible side effect of dasatinib is pulmonary arterial hypertension (Claudiani, Apperley, 2018). Afterward, EGFR protein is involved in cell growth and progression, including promoting angiogenesis, proliferation, metastasis, and inhibition in the apoptosis process. It was reported that high levels of EGFR have also been found in a variety of tumors such as breast, prostate, ovarian, colorectal, and gastric (Baselga, 2002). EGFR Inhibitors such as erlotinib can block the activation of EGFR proteins (Yuanita *et al*., 2019). These inhibitors interact with the ATP binding site through a Hydrogen bond, thereby blocking signal transduction (Ismail *et al*., 2016). Erlotinib is a well-known EGFR TKI approved as a treatment for non-small cell lung cancer (NSCLC) (da Cunha Santos, Shepherd, Tsao, 2011). Erlotinib exhibited potentially greater efficacy but significantly higher toxicities than icotinib and gefitinib (Liang *et al*., 2014). Therefore, imatinib and erlotinib as chemotherapy agents generate undesirable side effects by damaging the normal cells and can cause a multidrug resistance phenomenon (Hamza *et al*., 2022; Hirano *et al*., 2015).

Computational approaches, such as molecular docking and molecular dynamic simulations, are the most recent technologies for developing new anticancer agents. Those methods can be used at the molecular level to know the stability and interaction between the anticancer agent and the targeted protein. This information lets us evaluate the behavior of the ligand in the protein's binding site and elucidate its mechanism of action in the essential biochemical processes (McConkey, Sobolev, Edelman, 2002; Hospital *et al*., 2015). This method is routinely used to understand the drug-receptor interactions in the rational drug design (Vijesh *et al*., 2013). The lowest binding energy indicates the best conformation and the strongest interaction on the active site of the targeted protein (Mukesh, Rakesh, 2011). The new drug with the strongest interaction with the protein will be chosen to be synthesized in the laboratory and evaluated through biological assays. Consequently, the *in-silico* studies are less time-consuming, with fewer trials and errors and free usage of the chemicals, which greatly aids the drug development process.

The co-crystal structures of imatinib and erlotinib can be used to search for new inhibitors of PDGFR and EGFR proteins through the molecular docking study. From these structures, the interaction of the proteins with imatinib and erlotinib can be studied to design better inhibitor agents. It was reported that the interaction between protein and compound occurred primarily through the Hydrogen bond; thus, the design of the inhibitor must have a Hydrogen bond donor group that can interact with the amino acid residues of PDGFR and EGFR proteins. Hydrogen bond interaction with PDGFR and EGFR proteins was reported in our previous study by docking hydroxy thioxanthone derivatives (Hermawan *et al*., 2020). However, the inhibition activity of hydroxy thioxanthone derivatives is still lower than imatinib in PDGFR protein; thus, further modification of the hydroxy thioxanthone structure needs to be studied.

Xanthone derivatives containing the epoxy group have been reported for their remarkable anticancer activity (Woo *et al*., 2010). Psorospermin is a natural xanthone with hydroxy, methoxy, and epoxy groups that exhibit excellent anticancer activity against murine and human cancer cell lines (Kupchan, Streelman, Sneden, 1990; Na, 2009). Furthermore, the 1,3-dihydroxyxanthone with 2,3-epoxypropoxy groups at C-1 and C-3 positions have

potential as breast anticancer agents of MCF-7 cells. The additional 2,3-epoxypropoxy in the C-3 position was revealed with an IC_{50} value of 68.4 μM. Meanwhile, the additional 2,3-epoxypropoxy in the C-1 and C-3 positions drastically improve the IC_{50} value to 3.28 μM against MCF-7 (Woo *et al*., 2007). It was also reported that thioxanthone with a 2,3-epoxypropoxy substituent at the C-3 position of 1,3-dihydroxythioxanthone had better anticancer activity with IC_{50} of 50.2 μM against MCF7 cell (Woo *et al*., 2008). Although other studies have confirmed that synthesized thioxanthone derivatives with chloro substituent at the C-4 position can potentially act as breast anticancer agents of MCF-7 and MDA-MB-468 cells (Chen *et al*., 2019). Furthermore, it was investigated that adding one chloro and one hydroxyl group at the C-2 and C-4 positions of thioxanthone enhanced their anticancer activity against Hela, WiDr, T47D, and A549 cancer cells (Hermawan *et al*., 2022). Meanwhile, the additional bromo group at the C-4 position of 1,3-dihydroxyxanthone increases the inhibition activity against EGFR and PDGFR proteins (Hermawan *et al*., 2020). However, a molecular docking study, molecular dynamics simulation, and the calculation binding energy MM-PBSA of thioxanthone derivatives bearing with 2,3-epoxypropoxy, hydroxy, chloro, and bromo substituents have not been available as of today to the best of our knowledge. In light of the above findings, the molecular docking study and molecular dynamics simulation were conducted to investigate the inhibition mechanism, the interaction, and the stability of thioxanthone derivatives on the active site of PDGFR and EGFR proteins.

MATERIAL AND METHODS

Material

Two protein tyrosine kinases, *i.e.,* PDGFR (PDB ID: 1T46) and EGFR (PDB ID: 1M17), were downloaded from the Protein Data Bank database (www.rcsb.org). A series of thioxanthone derivatives with epoxy and halogen substituents (compound **A-J**) were used as ligands, and their chemical structures are shown in Figure 1.

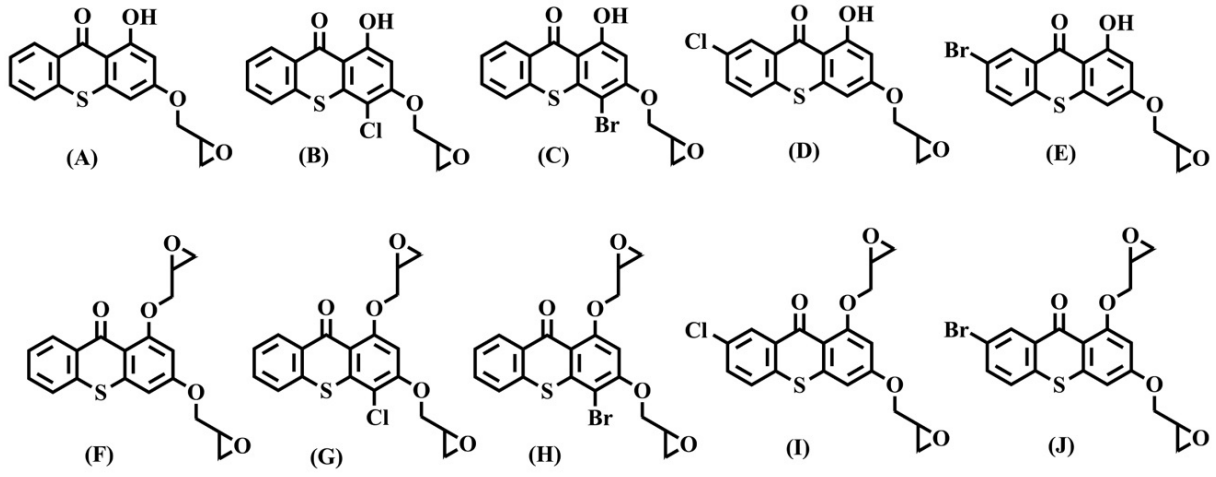

FIGURE 1 - The chemical structures of epoxy-thioxanthone derivatives in the molecular docking study.

Preparation of protein molecule and native ligand

PDGFR and EGFR proteins were isolated from all residues, such as water molecules and native ligands, using UCSF Chimera software (Pettersen *et al*., 2004). Afterward, their structures were saved in a PDB format file. The same method is used to isolate the native ligand, *i.e.,* imatinib (as the native ligand of PDGFR) and erlotinib (as the native ligand of EFGR). Both native ligands were cleaned from protein and water molecules and saved in a PDB format file.

Optimizing of epoxy thioxanthone derivatives

The three-dimensional (3D) epoxy-thioxanthones **A–J** structure was drawn using GaussView 5.0.8 software. Then, their structure was optimized using Gaussian-09 Revision D.01 software with a semi-empirical method and saved in the .pdb format (Frisch *et al*., 2013).

Redocking analysis and docking analysis

The redocking process was carried out on the active site of PDGFR and EGFR proteins with their respective native ligand (imatinib and erlotinib) using AutoDock4 software (Morris *et al*., 2009). The grid box was arranged within a 40 × 40 × 50 Å in the x, y, and z directions for PDGFR protein and 42 × 40 × 40 Å for EGFR protein. The Lamarckian Genetic Algorithm (LGA) method was utilized for the 40 runs. The protein structure was maintained in its rigid form, and the position of the ligand was flexible during the docking process. The success of redocking analysis is reflected in the root mean square deviation (RMSD) value, which shall be less than 2 Å (Huey *et al*., 2007). The molecular docking followed the same procedure as the redocking analysis in which the epoxy-thioxanthone derivatives (**A-J**) were docked in the protein binding site, which is known from the redocking analysis. The final molecular docking results were shown using Discovery Studio Visualizer (DSV) 2019 (Biovia, 2019).

Molecular dynamic simulations and MM-PBSA free energies calculation

Simulations were performed using GROMACS 2020 package (Hess *et al*., 2008; Pronk *et al*., 2013). The charmm36 force field was applied to conduct MD simulations off all complexes (Huang, MacKerell Jr, 2013). Topology parameters of all compounds were generated using the cgenff server (Pronk *et al*., 2013). PBC (periodic boundary condition) was performed as a small representative of the real system. Minimization energy was performed with the steepest descent for 1 ns; minimization was stopped when energy reached 100 kJ/mol. NVT and NPT ensemble were performed respectively to equilibrate the system for 1 ns each with dt 2 fs at 300 K and 1 atm using verlet cut-off. Parrinello-Rahman was used as pressure coupling at the NPT ensemble. System conditions were regulated as isotropic, PME (Particle Mesh Ewald) used for long-range electrostatic and v-rescale of modified Berensen thermostat were performed for temperature coupling (Verlet, 1967; Hünenberger, 2005; Martonák, Laio, Parrinello, 2003). MD production was performed for 50 ns under the same condition. RMSD (Root Mean Square Deviation), RMSF (Root Mean Square Fluctuation), RG (Radius of Gyration), and Hydrogen bond were taken from MD production. Furthermore, the Molecular mechanics Poisson-Boltzmann surface area (MM-PBSA) studies were conducted to determine free energy such as van der Waals, electrostatic, polar salvation, SASA, and binding energies. The calculation of free binding energies adopted the g_mmpbsa package (Kumari *et al*., 2014). The ligand-protein MD trajectory data and parameter file were used to execute the g_mmpbsa with single-step calculation.

Physicochemical and ADMET properties

Using Discovery Studio, all compounds were converted into smiles format and then uploaded one by one to the pkCSM server (Pires, Blundell, Ascher, 2015). The determination of physicochemical and ADMET properties was conducted by choosing the ADMET menu. Afterward, the pkCSM showed the data for each compound, including Lipinski's rule of five, adsorption, distribution, metabolism, excretion, and toxicity.

RESULTS AND DISCUSSION

Redocking analysis into different protein tyrosine kinase

A molecular docking study of ten epoxy-thioxanthones was carried out on two types of tyrosine kinase, *i.e.,* PDGFR and EGFR proteins. The epoxy-thioxanthone derivatives were docked into the active site of each protein tyrosine kinase to study the possible interaction as the tyrosine kinase inhibitor agents.

To reach that goal, we first performed the redocking process to validate the binding position and adjust the parameters of the docking process (Cosconati *et al*., 2010). Imatinib, as the native ligand, was docked into PDGFR protein, and it showed the lowest RMSD of 0.61 Å with a binding energy of −13.36 kcal/mol. On the other hand, the redocking of erlotinib ligand into the EGFR protein yielded the lowest RMSD value of 1.59 Å with a binding energy of -7.05 kcal/mol. Redocking of these native ligands was successfully performed as the RMSD values were less than 2 Å, demonstrating that the experimental parameters were accurate for the docking process of epoxy-thioxanthone derivatives.

Molecular docking study of epoxy-thioxanthone derivatives with PDGFR protein

Molecular docking of epoxy-thioxanthones **A-J** was conducted using the same parameters from the redocking analysis. All compounds (**A-J**) were fixed to have the same position as imatinib and docked into 30 possible ligand conformations in PDGFR protein. The molecular docking experiment resulted in several parameters, such as binding energy, inhibition constant (Ki), Hydrogen bond and other intermolecular forces, and RMSD value. The molecular docking result of epoxy-thioxanthone **A-J** is shown in Table I. The molecular docking experiment is valid and reliable when the RMSD value is less than 2Å (Huey *et al*., 2007). The lower binding energy indicates the compound has higher inhibition activity against tyrosine kinase protein (Dolatkhah *et al*., 2017). On the other hand, a lower Ki value represents a more preferred ligand-protein interaction (Heh *et al*., 2013). Visualizing Hydrogen bonds and other intermolecular forces is pivotal to evaluating the mechanism of action of epoxy-thioxanthone as a tyrosine kinase inhibitor.

The molecular docking result with PDGFR protein (Table I) showed that all epoxy-thioxanthone derivatives have the RMSD value of 0.95 to 1.75 Å; thus, the obtained molecular docking results were reliable enough. The binding energy of all epoxy-thioxanthone derivatives (-7.12 to -9.81 kcal/mol) was higher than imatinib as the native ligand (-13.36 kcal/mol). However, it is worth noting that the epoxy-thioxanthone (-7.12 to -9.81 kcal/mol) has stronger binding energies than hydroxy-thioxanthone (-7.10 to -8.57 kcal/mol), which is remarkable (Hermawan *et al*., 2020).

From the binding energy data, adding either chloro or bromo functional group on the monoepoxy-thioxanthone lowers the binding energy value. The addition of chloro substituent at the 4- and 7-position of monoepoxy-thioxanthone decreased the binding energy value of compound **A** (-8.93 kcal/mol) to -9.26 and -9.62 kcal/mol on compounds **B** and **D**, respectively. On the other hand, the addition of bromo substituent at 4- and 7-position of monoepoxy-thioxanthone decreased the binding energy value of compound **A** (-8.93 kcal/mol) to -9.27 and -9.81 kcal/mol on compound **C** and **E**, respectively. This result demonstrates that the bromo substituent has a higher biological activity as a PDGFR Tyrosine kinase inhibitor than the chloro substituent on monoepoxy-thioxanthones. Furthermore, the halogen substituent at the 7-position has lower binding energy than the 4-position of monoepoxy-thioxanthones.

TABLE I - Molecular docking results of compounds **A-J** and imatinib with PDGFR protein

Compound	RMSD (Å)	Binding Energy (kcal/mol)	Ki (μM)	Hydrogen Bond (Å)
A	1.26	-8.93	0.284	Cys673 (2.055) Asp810 (1.718)
B	1.31	-9.26	0.162	Cys673 (2.067) Asp810 (1.849)

TABLE I - Molecular docking results of compounds **A-J** and imatinib with PDGFR protein

Compound	RMSD (Å)	Binding Energy (kcal/mol)	Ki (μM)	Hydrogen Bond (Å)
C	1.63	-9.27	0.159	Cys673 (1.762) Asp810 (1.993) Glu671 (1.921)
D	1.57	-9.62	0.088	Cys673 (2.162) Glu671 (2.005) Asp810 (1.862)
E	0.95	-9.81	0.064	Cys673 (1.861) Glu671 (1.958)
F	1.48	-8.67	0.433	Cys673 (2.230) Asp677 (2.231)
G	1.75	-7.12	6.050	Asn680 (1.871)
H	1.25	-7.92	1.520	Lys593 (1.879) Asn680 (2.068)
I	1.55	-9.43	0.123	Lys593 (1.750) Asp677 (2.060)
J	1.44	-9.74	0.072	Lys593 (1.178) Asp677 (1.790)
Imatinib	0.61	-13.36	0.0002	Asp810 (1.877) Cys673 (1.874)

It was found that the binding energy of diepoxy-thioxanthone **F** (-8.67 kcal/mol) was higher than monoepoxy-thioxanthone **A** (-8.93 kcal/mol), probably due to the steric effect on the active site of PDGFR protein. The addition of chloro- and bromo- substituent at 4-position of diepoxy-thioxanthone increased the binding energy value of compound **F** (-8.67 kcal/mol) to -7.12 and -7.92 kcal/mol on compound **G** and **H**, respectively. The steric effect might cause this phenomenon. On the other hand, the addition of chloro- and bromo- substituent at the 7-position of diepoxy-thioxanthone decreased the binding energy value of compound **F** (-8.67 kcal/mol) to -9.43 and -9.74 kcal/mol on the compound **I** and **J**, respectively. This result demonstrates that the bromo substituent has a higher biological activity as a PDGFR Tyrosine kinase inhibitor than the chloro substituent on diepoxy-thioxanthones. The halogen substituent at the 7-position has lower binding energy than the 4-position of diepoxy-thioxanthones. These trends were the same for the monoepoxy-thioxanthone derivatives. It was also found that a lower binding energy led to a lower Ki value for both monoepoxy- and diepoxy-thioxanthones. Therefore, compound **E** was the most potential candidate as a tyrosine kinase inhibitor against PDGFR protein with binding energy and Ki value of -9.81 kcal/mol and 0.064 μM, respectively.

To discuss the intermolecular interactions of epoxy-thioxanthone derivatives on the active site of PDGFR protein, we limited the discussion to the epoxy-thioxanthones with a binding energy value lower than -9.40 kcal/mol, i.e., compound **D** (-9.62 kcal/mol), compound **E** (-9.81 kcal/mol), compound **I** (-9.43 kcal/mol), and compound **J** (-9.74 kcal/mol). The interactions formed between all epoxy-thioxanthone compounds with PDGFR protein were Hydrogen bond, van der Waals, π-sigma, and π-alkyl interactions, as can be shown in Figure 2 from compound **E** as the representative epoxy-thioxanthone compound. The Hydrogen bond interaction of compounds **D**

and **E** occurred with the amino acid residues of Cys673 and Glu671 (Table I). Meanwhile, the Hydrogen bond interaction of compounds **I** and **J** occurred with the amino acid residues of Lys593 and Asp677 (Table I). Both compounds **D** and **E** have similar Hydrogen bonds with Cys673 amino acid residue, as also found in imatinib as the native ligand. In contrast, this Hydrogen bond was absent in the compounds **I** and **J**. The binding energy of compound **E** (-9.81 kcal/mol) was lower than compound **D** (-9.62 kcal/mol) due to the shorter Hydrogen bond interaction of compound **E** (1.861 Å) than compound **D** (2.162 Å) with Cys673 amino acid residue of PDGFR protein. Even though the compound **E** (1.861 Å) has a slightly shorter Hydrogen bond than imatinib (1.877 Å) with Cys673, the binding energy of imatinib was still lower due to the presence of a Hydrogen bond with Asp810. The interaction with Asp810 and Cys673 is pivotal for the inhibition activity of PDGFR protein (Hermawan *et al*., 2020).

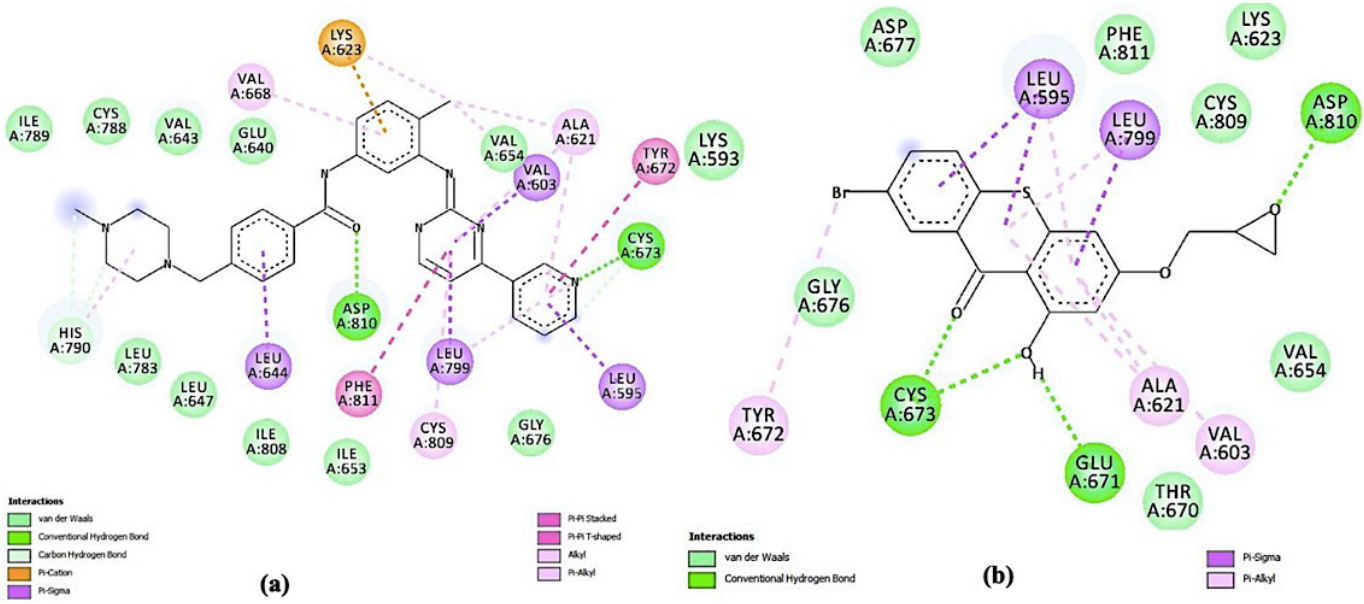

FIGURE 2 - The visualization of intermolecular interactions towards PDGFR protein in 2D (a) Imatinib and (b) compound **E.**

Molecular docking study of epoxy-thioxanthone derivatives with EGFR protein

The molecular docking result with EGFR protein (Table II) showed that all epoxy-thioxanthone derivatives have the RMSD value in a range of 0.85-1.75 Å; thus, the obtained molecular docking results were reliable enough. The binding energy of all epoxy-thioxanthone derivatives (-7.24 to -8.06 kcal/mol) was lower than erlotinib as the native ligand (-7.05 kcal/mol), which is remarkable. Furthermore, the epoxy-thioxanthone (-7.24 to -8.06 kcal/mol) has stronger binding energy than hydroxy-thioxanthone (-6.23 to -7.25 kcal/mol), demonstrating that epoxy-thioxanthone derivatives are potential tyrosine kinase inhibitor candidate against EGFR protein (Hermawan *et al*., 2020).

From the binding energy data, adding either chloro or bromo functional group on the monoepoxy-thioxanthone lowers the binding energy value. The addition of chloro substituent at the 4- and 7-position of monoepoxy-thioxanthone decreased the binding energy value of compound **A** (-7.46 kcal/mol) to -7.56 and -7.94 kcal/mol on compounds **B** and **D**, respectively. On the other hand, the addition of bromo substituent at 4- and 7-position of monoepoxy-thioxanthone decreased the binding energy value of compound **A** (-7.46 kcal/mol) to -7.61 and -8.06 kcal/mol, respectively, on compound **C** and **E**. This result demonstrates that the bromo

substituent has a higher biological activity as an EGFR tyrosine kinase inhibitor than the chloro substituent on monoepoxy-thioxanthones. Furthermore, the halogen substituent at the 7-position has lower binding energy than the 4-position of monoepoxy-thioxanthones.

TABLE II - Molecular docking result of compounds **A-J** and erlotinib with EGFR protein

Compound	RMSD (Å)	Binding Energy (kcal/mol)	Ki (μM)	Hydrogen Bond (Å)
A	0.98	-7.46	3.39	Met769 (1.693) Thr766 (2.171) Asp831 (1.957)
B	0.85	-7.56	2.87	Met769 (1.793) Gln767 (2.074) Asp831 (1.968)
C	1.06	-7.61	2.63	Met769 (1.726) Asp831 (2.104)
D	0.91	-7.94	1.53	Met769 (1.743) Thr831 (2.047)
E	0.99	-8.06	1.23	Met769 (1.783) Thr831 (1.972)
F	1.57	-7.33	4.24	Met769 (1.796) Thr830 (2.202)
G	1.75	-7.24	4.94	Met769 (1.797) Lys721 (1.968)
H	1.5	-7.52	3.10	Met769 (1.914) Thr830 (1.990) Lys721 (1.971)
I	1.48	-7.85	1.76	Met769 (2.021) Lys721 (2.229) Thr830(1.778)
J	1.42	-7.92	1.57	Met769 (2.106) Lys721 (1.639)
Erlotinib	1.59	-7.05	6.77	Met769 (1.659) Cys773 (2.064)

It was also found that the binding energy of diepoxy-thioxanthone **F** (-7.33 kcal/mol) was slightly higher than monoepoxy-thioxanthone **A** (-7.46 kcal/mol) probably due to the steric effect on the active site of EGFR protein. The addition of chloro-substituent at the 4-position of diepoxy-thioxanthone slightly increased the binding energy value of compound **F** (-7.33 kcal/mol) to -7.24 kcal/mol on compound **G**. In contrast, the addition of bromo-substituent at the 4-position of diepoxy-thioxanthone decreased the binding energy value of compound **F** (-7.33 kcal/mol) to -7.52 kcal/mol on compound **H**. On the other hand, the addition of chloro- and bromo- substituent at the 7-position of diepoxy-thioxanthone decreased the binding energy value of compound **F** (-7.33 kcal/mol) to -7.85 and -7.92 kcal/mol on compound **I** and **J**, respectively. This result demonstrates that the bromo substituent

has a higher biological activity as an EGFR tyrosine kinase inhibitor than the chloro substituent on diepoxy-thioxanthones. The halogen substituent at the 7-position has lower binding energy than the 4-position of diepoxy-thioxanthones. It was also found that a lower binding energy led to a lower Ki value for both monoepoxy- and diepoxy-thioxanthones. These trends were the same for the molecular docking data of epoxy-thioxanthone derivatives against PDGFR protein. Therefore, compound **E** was the most potential candidate as a tyrosine kinase inhibitor against EGFR protein with binding energy and Ki value of -8.06 kcal/mol and 1.23 μM, respectively.

To discuss the intermolecular interactions of epoxy-thioxanthone derivatives on the active site of EGFR protein, we limited the discussion to the epoxy-thioxanthones with a binding energy value lower than -7.80 kcal/mol, i.e., compound **D** (-7.94 kcal/mol), compound **E** (-8.06 kcal/mol), compound **I** (-7.85 kcal/mol), and compound **J** (-7.92 kcal/mol). The interactions formed between all epoxy-thioxanthone compounds with EGFR protein were Hydrogen bond, van der Waals, carbon-hydrogen, π-sigma, alkyl, and π-alkyl interactions as can be shown in Figure 3 from compound **E** as the representative epoxy-thioxanthone compound. The Hydrogen bond interaction of compounds **D** and **E** occurred with the amino acid residues of Met769 and Thr831 (Table II). Meanwhile, the Hydrogen bond interaction of compounds **I** and **J** occurred with the amino acid residues of Met769 and Lys721 (Table II). The compounds **D**, **E**, **I**, and **J** have similar hydrogen bonds with Met769 amino acid residue, as also found in erlotinib as the native ligand. The lower binding energy of epoxy-thioxanthones than erlotinib was caused by the Hydrogen bond of epoxy-thioxanthones with Met769 and additional Hydrogen bonds with other amino acid residues, such as Thr766, Asp831, Gln767, Asp831, Thr831, Thr830, and Lys721. These amino acid residues of EGFR have been reported to be crucial to the inhibition mechanism (Singh, Bast, 2014). The binding energy of compound **E** (-8.06 kcal/mol) was lower than compound **I** and **J** (-7.85 and -7.92 kcal/mol) due to the shorter Hydrogen bond interaction of compound **E** (1.783 Å) than compound **I** and **J** (2.021 and 2.106 Å) with Met769 amino acid residue of EGFR protein. Even though compound **E** (1.783 Å) has a slightly longer Hydrogen bond than compound **D** (1.743 Å) with Met769, compound **E** (1.972 Å) generated a shorter Hydrogen bond with Thr831 than compound **D** (2.047 Å). The interaction with Met769 seems pivotal for the inhibition activity of EGFR protein; however, further study is required to confirm this phenomenon. Furthermore, the compounds **D**, **E**, **I**, and **J**, which form the most stable complex with the EGFR protein, were further analyzed for molecular dynamics simulations.

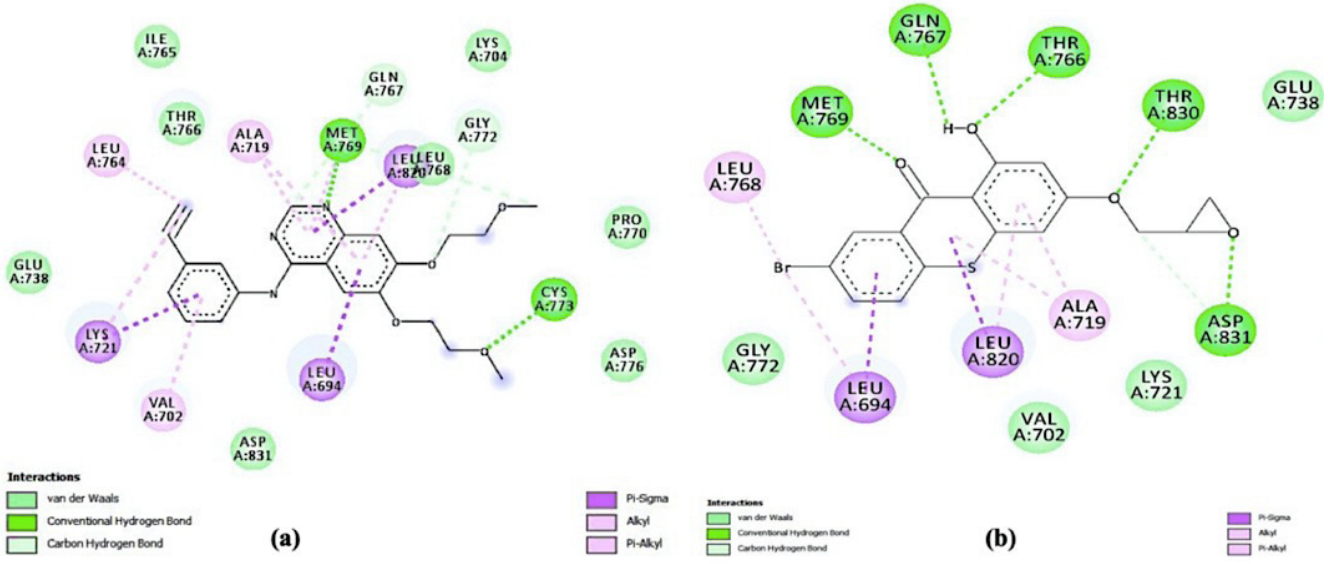

FIGURE 3 - The visualization of intermolecular interactions towards EGFR protein in 2D (a) Erlotinib and (b) compound **E.**

Molecular dynamic simulations

To provide a distinct picture of the dynamics of the ligand and protein in the water solvent, 50 ns of molecular dynamic simulations were conducted between the EGFR protein and its native ligand, compounds **D**, **E, I**, and **J**. The simulation results provide useful information, including the Root Mean Square deviation (RMSD) of each ligand and complex with protein, the Root Mean Square Fluctuation (RMSF) of the simulation system backbone, the Radius of Gyration (Rg) of the ligand and protein, and the hydrogen bonds that form between the ligand and the amino acid of the protein.

Figure 4 displays the ligand and complex's RMSD values throughout the simulation. Each ligand's RMSD varies between 0.5 to 2 Å. This suggests that the ligand within the protein's active site does not undergo significant movement; instead, it stays in the active site throughout the simulation, resulting in interactions between the ligand and the active site continuing for 50 ns. This might also suggest that the ligand inhibits the activity of the EGFR protein. In the meantime, the RMSD value of the complex yields quite intriguing values, with the RMSD value of the complex containing the erlotinib and compound **J** falling between 2 and 4 Å (Figure 4b). According to these findings, the complex containing the ligand in the active site does not exhibit significant movement, unlike the complex containing the ligands **D, E**, and **I**, where the RMSD values tend to be high.

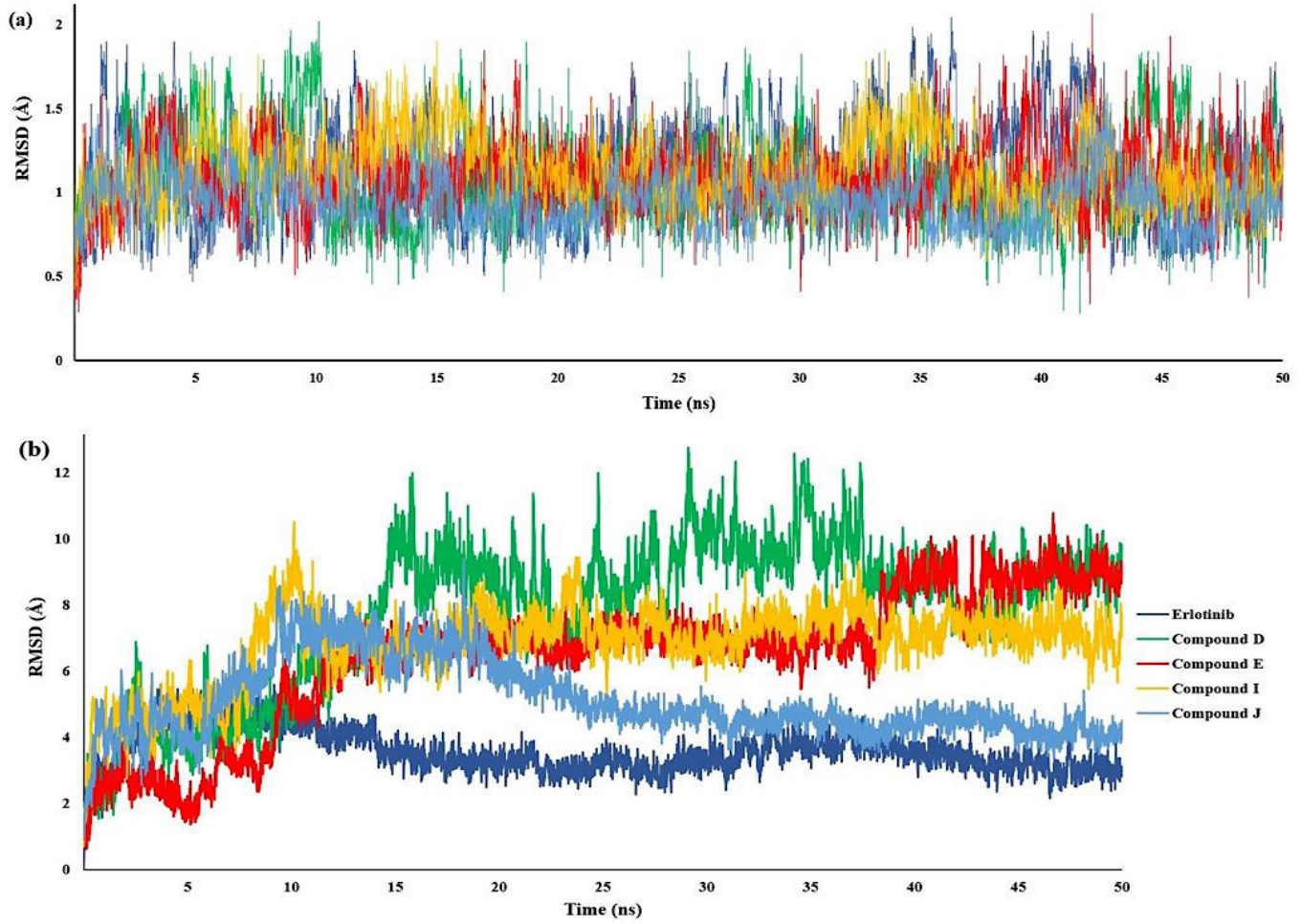

FIGURE 4 - (a) RMSD ligand and (b) RMSD complex.

This RMSD value is also corroborated by the RMSF value (Figure 5a), demonstrating the backbone system. The RMSF graph revealed that compounds (**D**, **E**, **I**, and **J)** had similar patterns of amino acid fluctuation with erlotinib. This suggested that compounds (**D**, **E**, **I,** and **J)** had similar patterns of binding interactions against the EGFR protein. Nevertheless, compounds **D** and **E** displayed a higher RMSF value than erlotinib, compounds **I** and **J**. This finding implies that compounds **D** and **E** fluctuate significantly more than erlotinib on the active side.

As shown in Figure 5b, the protein from compound **D** has a high Rg at the start of the simulation; this value remains high around 2.4 to 2.6 nm but diminishes after the simulation has lasted longer than 30 ns. Meanwhile, the protein containing compounds **E**, **I**, **J,** and erlotinib has a Rg value up to 2.2 nm, whereas compound **E** also has a high Rg value between 2.2 and 2.3 nm; however, this value only lasts for 10 ns. Afterward, on the rest of the simulation time, the Rg value of those ligands is constant at 2.05-2.15 nm. Compared with other compounds, compound **J** showed the lowest Rg value, implying that compound **J** is more compact and stable than the other ligands.

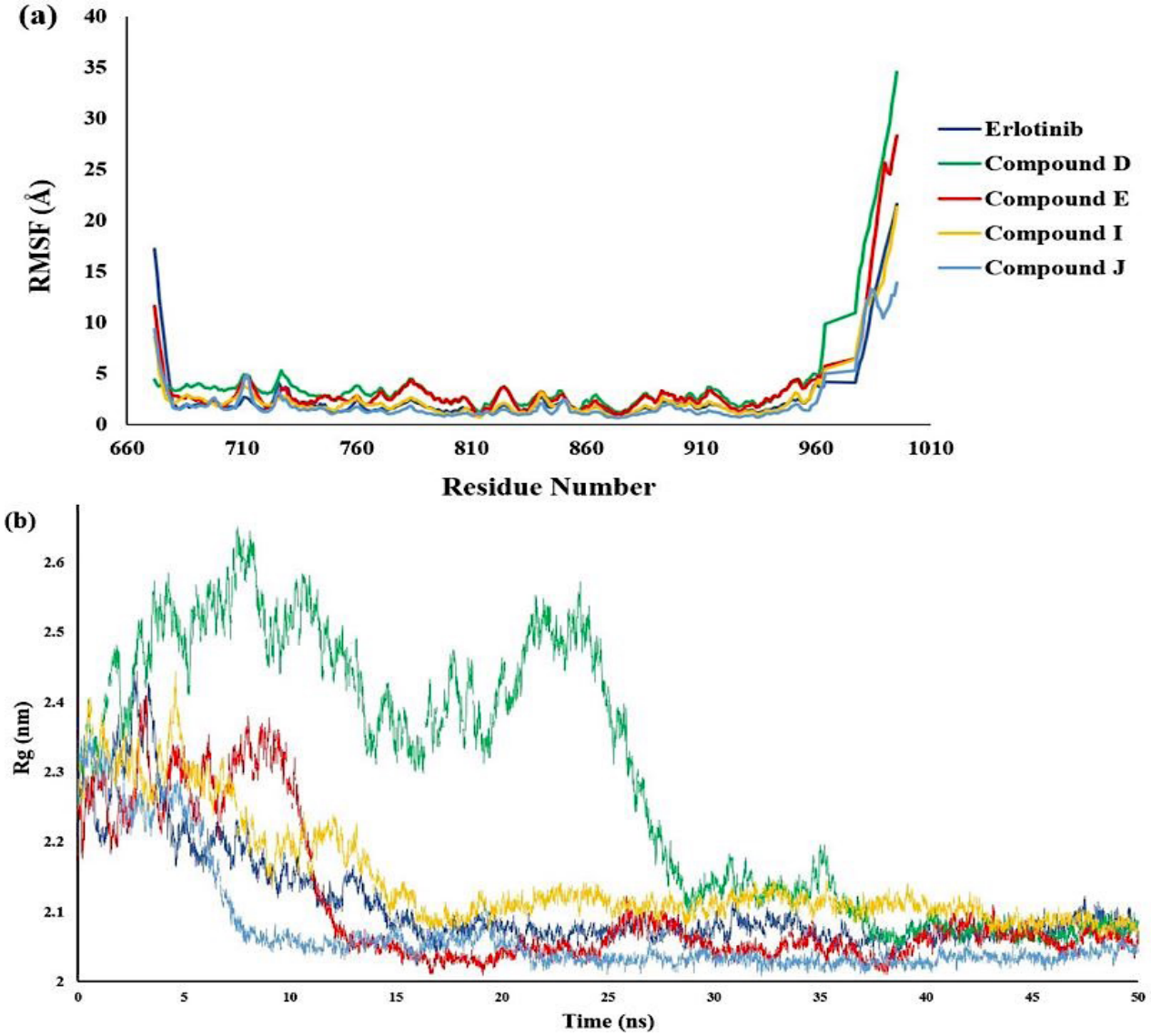

FIGURE 5 - (a) RMSF of erlotinib compounds **D**, **E**, **I** and **J** and (b) Radius of gyration compounds **D**, **E**, **I, J** and erlotinib.

Through molecular dynamics simulations, as seen in Figure 6, it is also possible to understand how hydrogen bonds between ligands and amino acids in the protein's active site interact. In the erlotinib ligand, the maximum number of 2 hydrogen bonds formed during the simulation occurred, with an average of 1 bond formed; however, under some circumstances, no hydrogen bonds are formed. This is in contrast to compound **D**, which forms the most hydrogen bonds (6 bonds), while under some circumstances, 4-5 bonds are formed during the simulation, and compound **E**, which forms the most hydrogen bonds 5, with an average of 2-3 bonds. Meanwhile, the most hydrogen bonds formed in compound **I** is 4, under some circumstances 2 bonds, and compound **J** forms at most 3 hydrogen bonds, with an average of 2-3 bonds formed during the simulation.

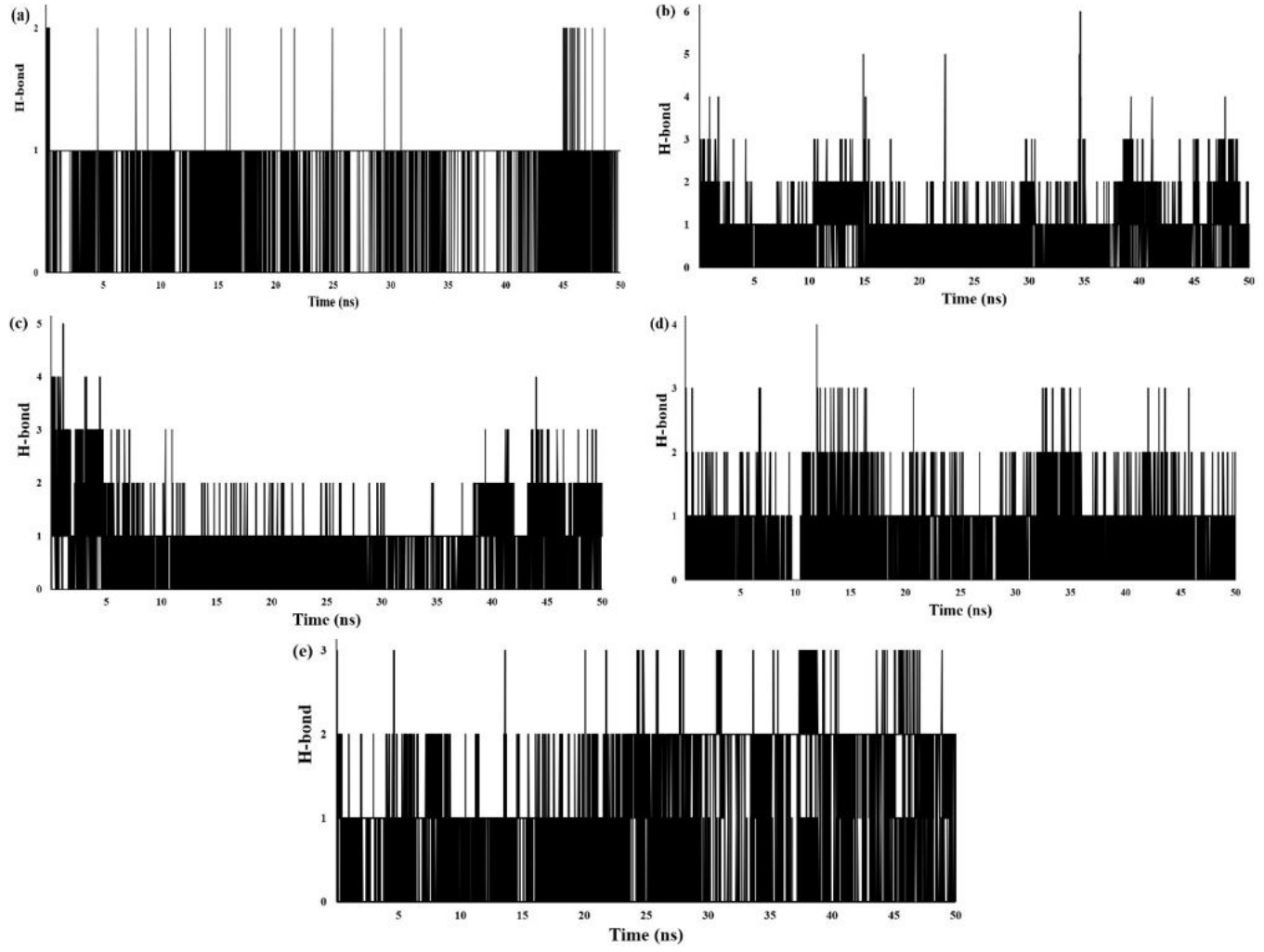

FIGURE 6 - Hydrogen bond of (a) erlotinib, (b) Compound **D**, (c) Compound **E**, (d) Compound **I**, (e) Compound **J.**

MM-PBSA: Calculation and analysis of binding free energy

The binding energy is the total of all noncovalent interactions. The binding energies of all compounds and erlotinib were calculated using the MM-PBSA method. The Van der Waal's energy, electrostatic energy, polar solvation energy, SASA energy, and binding energy were determined for the last 10 ns of the MD trajectory. As shown in Table III, compounds **D**

(-19.29 kcal/mol), **E** (-21.52 kcal/mol), **I** (-26.56 kcal/mol) and **J** (-29.35 kcal/mol) had lower binding energy than erlotinib (-8.25 kcal/mol). It suggests that the complex with the EGFR protein of those compounds is more stable.

TABLE III - MM-PBSA binding energy of compounds **D**, **E**, **I**, **J** and erlotinib

Compound	Van der waal's energy (kcal/mol)	Electrostatic energy (kcal/mol)	Polar solvation energy (kcal/mol)	SASA energy (kcal/mol)	Binding energy (kcal/mol)
D	-35.80 ± 2.71	-5.29 ± 2.88	25.45 ± 4.06	-3.65 ± 0.25	-19.29 ± 2.74
E	-33.42 ± 2.88	-6.17 ± 2.07	21.31 ± 3.87	-3.48 ± 0.30	-21.52 ± 3.27
I	-42.75 ± 2.37	-6.64 ± 2.39	26.92 ± 4.19	-4.09 ± 0.23	-26.56 ± 3.54
J	-43.32 ± 2.93	-10.71 ± 3.04	29.03 ± 5.73	-4.34 ± 0.24	-29.35 ± 3.91
Erlotinib	-37.91 ± 2.67	-6.72 ± 2.13	41.17 ± 4.00	-4.79 ± 0.25	-8.25 ±3.06

Physicochemical and ADMET properties

Prediction of physicochemical and ADMET properties is essential for drug discovery, especially to determine the ability of small molecule drugs in metabolism, distribution, absorption, extraction, and toxicology. The physicochemical and ADMET properties results were obtained from the pkCSM web server (Table IV). Based on Lipinski's rule of five, a drug should have molecular weight < 500 Da, the logarithm of the octanol-water partition coefficient (log P) < 5, rotatable bonds (ROTB) < 10, hydrogen bond acceptor (HBA) < 10, hydrogen bond donor (HBD) < 5, and polar surface area (PSA) < 140 Å (Lipinski, 2004). Table IV shows that the physicochemical properties of all compounds **(D**, **E**, **I**, and **J)** fulfill the Lipinski rule of five parameters.

Caco-2 is frequently utilized in the absorption parameters as an in vitro model of the human mucosa for predicting medication absorption when applied orally. A drug has been found to have high Caco-2 permeability with values > 0.90. Subsequently, the intestinal absorption (IA) properties predict the percentage of a drug absorbed through the human intestines. Less than 30% absorption is considered poor, whereas more than 80% is considered good. Table IV shows that compounds **D**, **E**, **I,** and **J** fulfill the absorption parameters, including Caco-2 permeability and intestinal absorption. The distribution parameters of drugs were determined by VDss value, BBB permeability, and CNS permeability. Log VDss < -0.15 implies low VDss, whereas log VDss > 0.45 suggests high VDss. A higher VDss value implies that the medicine will be more dispersed in tissue than in plasma. Afterward, the brain readily absorbs drugs with a logBB > 0.3, whereas those with a logBB > -1 are poorly distributed there. Another approach is the blood-brain permeability-surface area product (logPS), also known as CNS permeability. All compounds (**D, E, I,** and **J**) fulfill those parameters.

The metabolism properties showed that all epoxy-thioxanthenes (**D**, **E**, **I**, and **J**) were unsuitable as CYP2D6 substrates and more likely to act as CYP3A4 substrates. These two substrates are primarily essential for Cytochrome P450 metabolism. Cytochrome P450 is a crucial detoxifying enzyme in the human body, primarily found in the liver. Furthermore, the excretion parameters showed that all compounds (**D, E, I,** and **J**) had a total clearance value of 0.283-0.542. Meanwhile, those compounds did not comply with the Renal Organic Cation Transporter 2 (OCT2) parameter. The OCT2 parameter represents the disposition and clearance of the drug.

The maximum recommended tolerated dose (MRTD) is the level of a chemical hazardous dosage limit

in humans. An MRTD medication with a value less than or equal to 0.477 is regarded as low. All compounds (**D, E, I,** and **J**) had low MRTD values. Those compounds showed no inhibition activity towards hERG I. The hepatoxicity parameter is associated with harmed liver and predicted values for thioxanthones **D** and **E** had no effect on the liver. Further, compounds **D, E, I,** and **J** do not affect the skin.

TABLE IV - Physicochemical and ADMET properties of compounds **D**, **E**, **I**, and **J**

	Properties	Compound			
		D	**E**	**I**	**J**
Physicochemical	Molecular weight	334.780	379.231	390.844	435.295
	log P	3.5513	3.6604	3.6233	3.7324
	Rotatable bond	3	3	6	6
	H-bond acceptor	5	5	6	6
	H-bond donor	1	1	0	0
	Surface area	134.021	137.585	157.543	161.107
Absorption	Caco-2 permeability	1.235	1.24	1.019	1.017
	Intestinal absorption	93.967	93.9	96.937	96.87
	Skin permeability	-2.797	-2.797	-2.744	-2.744
Distribution	VDss	0.097	0.144	0.243	0.26
	BBB permaebility	0.085	0.084	0.037	0.036
	CNS permaebility	-2.089	-2.066	-2.397	-2.375
Metabolism	CYP2D6 substrate	No	No	No	No
	CYP3A4 substrate	Yes	Yes	Yes	Yes
	CYP1A2 inhibitor	Yes	Yes	Yes	Yes
	CYP2C19 inhibitor	Yes	Yes	Yes	Yes
	CYP2C9 inhibitor	Yes	Yes	Yes	Yes
	CYP2D6 inhibitor	No	No	No	No
	CYP3A4 inhibitor	Yes	Yes	No	Yes
Excretion	Total clearance	0.305	0.283	0.542	0.520
	Renal OCT2 substrate	No	No	No	No
Toxicity	Max. Tolerated dose	0.276	0.278	-0.015	-0.009
	hERG I inhibitor	No	No	No	No
	hERG II inhibitor	Yes	Yes	No	No
	Hepatoxicity	No	No	Yes	Yes
	Skin sensitisation	No	No	No	No

CONCLUSIONS

The Molecular docking of thioxanthone derivatives (**A-J**) was studied to investigate the inhibition mechanism and the interaction of thioxanthone derivatives compounds bearing epoxy and halogen (Cl, Br) substituents against PDGFR and EGFR proteins. The results showed that ten thioxanthone derivatives have binding energy ranging from -7.12 to -9.81 kcal/mol for PDGFR protein and -7.24 to -8.06 kcal/mol for EGFR protein. It was found that epoxy-thioxanthone derivatives (**A-J**) gave a stronger interaction in EGFR protein than PDGFR protein. The molecular docking study in EGFR protein revealed that all epoxy-thioxanthones gave lower binding energy than native ligands (erlotinib), demonstrating that these compounds had better inhibitor activity for EGFR protein, which is remarkable. The molecular dynamics 50 ns simulation revealed that compounds **D**, **E**, **I**, and **J** had comparable EGFR protein stability to erlotinib. Meanwhile, the binding energy of MM-PBSA compounds was lower than that of erlotinib. Thioxanthones **D**, **E**, **I**, and **J** in physicochemical properties prediction fulfill Lipinski's rule parameters. In ADMET calculation, those compounds also fulfill the adsorption parameter and some of the distribution, metabolism, excretion, and toxicity tests. In conclusion, compounds **D**, **E**, **I**, and **J** are potential candidates for novel anticancer drugs, as further experimental *in vitro* and *in vivo* assays are required to prove their efficacy.

ACKNOWLEDGEMENTS

We are gratefully thankful to the Research Organization Health, National Research and Innovation Agency (BRIN) Indonesia for the financial support to research Rumah Program Purwarupa Bahan Baku Obat Terapi Terarah. The authors also sincerely thank for the Gaussian 09 licenses provided by Austrian-Indonesian Centre (AIC) for computational chemistry at Universitas Gadjah Mada.

REFERENCES

Abouantoun TJ, MacDonald TJ. Imatinib blocks migration and invasion of medulloblastoma cells by concurrently inhibiting activation of platelet-derived growth factor receptor and transactivation of epidermal growth factor receptor. Mol Cancer Ther. 2009;8(5):1137–1147.

Baselga J. Why the epidermal growth factor receptor? The rationale for cancer therapy. Oncologist. 2002;7(4):2–8.

Biovia DS. Discovery Studio Visualizer. San Diego: 2019.

Chen CL, Chen TC, Lee CC, Shih LC, Lin CY, Hsieh YY, et al. Synthesis and evaluation of new 3-substituted-4-chloro-thioxanthone derivatives as potent anti-breast cancer agents. Arab J Chem. 2019;12(8):3503–3516.

Claudiani S, Apperley JF. The argument for using imatinib in CML. Hematology Am Soc Hematol Educ Program. 2018;2018(1):161–167.

Cosconati S, Forli S, Perryman AL, Harris R, Goodsell DS, Olson AJ. Virtual screening with AutoDock: theory and practice. Expert Opin Drug Discov. 2010;5(6):597–607.

Coban O, Degim A. Development and validation of highly selective method for the determination of imatinib mesylate and dexketoprofen trometamol combination in three different media. Braz J Pharm Sci. 2020;56:e18583.

da Cunha Santos G, Shepherd FA, Tsao MS. EGFR mutations and lung cancer. Annu Rev Pathol. 2011;6:49–69.

Dolatkhah Z, Javanshir S, Sadr AS, Hosseini J, Sardari S. Synthesis, molecular docking, molecular dynamics studies, and biological evaluation of 4H-chromone-1,2,3,4-tetrahydropyrimidine-5-carboxylate derivatives as potential antileukemic agents. J Chem Int Model. 2017;57(6):1246–1257.

Frisch MJ, Trucks GW, Schlegel HB, Scuseria GE, Robb MA, Cheeseman JR, et al. *Gaussian-09 Revision D.01*. Wallingford CT: Gaussian Inc; 2013.

Hamza MS, Shouman SA, Abdelfattah R, Moussa HS, Omran MM. Determination of the Cut-off Value for Imatinib Plasma Levels Linked to Occurrence of Bone Pain in CML Patients. Drug Des Devel Ther. 2022;16:1595–1604.

Heh CH, Othman R, Buckle MJC, Sharifuddin Y, Yusof R, Rahman NA. Rational discovery of dengue type 2 non-competitive inhibitors. Chem Biol Drug Des. 2013;82(1):1–11.

Hermawan F, Jumina J, Pranowo HD. Design of thioxanthone derivatives as potential tyrosine kinase inhibitor: A molecular docking study. Rasayan J Chem. 2020;13(4):2626–2632.

Hermawan F. Jumina, Pranowo HD, Sholikhah EN, Iresha MR. Molecular docking approach for design and synthesis of thioxanthone derivatives as anticancer agents. ChemistrySelect. 2022;7:e202203076.

Hess B, Kutzner C, van der Spoel D, Lindahl E. GROMACS 4: Algorithms for highly efficient,load-balanced, and

scalable molecular simulation. J Chem Theory Comput. 2008;4(3):435–447.

Hirano T, Yasuda H, Tani T, Hamamto J, Oashi A, Ishioka K, et al. In vitro modeling to determine mutation specificity of EGFR tyrosine kinase inhibitors against clinically relevant EGFR mutants in non-small-cell lung cancer. Oncotarget. 2015;6(36):38798–38803.

Hospital A, Goni JR, Orozco M, Gelpi JL. Molecular dynamics simulations: advances and applications. Adv Appl Bioinform Chem. 2015;8:37–47.

Huang J, MacKerell Jr AD. CHARMM36 all-atom additive protein force field: validation based on comparison to NMR data. J Comput Chem. 2013;34(25):2135–2145.

Huey R, Morris GM, Olson AJ, Goodsell DS. A semiempirical free energy force field with charge-based desolvation. J Comput Chem. 2007;28(6):1145–1152.

Hünenberger PH. Thermostat algorithms for molecular dynamics simulations. Adv. Polymer. Sci. 2005;173:105–149.

Ismail RSM, Ismail NSM, Abuserii S, El-Ella DAA. Recent advances in 4-aminoquinazoline based scaffold derivatives targeting EGFR kinases as anticancer agents. Future J Pharm Sci. 2016;2:09–19.

Kanaan R, Strange C. Use of multitarget tyrosine kinase inhibitors to attenuate platelet-derived growth factor signalling in lung disease. Eur Respir Rev. 2017;26(146):170061.

Karabacak M, Altıntop MD, Çiftçi HI, Koga R, Otsuka M, Fujita M, et al. Synthesis and evaluation of new pyrazoline derivatives as potential anticancer agents. Molecules. 2015;20(10):19066–19084.

Kumari R, Kumar R, Lynn A. g_mmpbsa—a GROMACS tool for high-throughput MM-PBSA calculations. J. Chem. Inf. Model. 2014;54(7):1951–1962.

Kupchan, SM, Streelman DR, Sneden AT. Psorospermin, a new antileukemic xanthone from Psorospermum febrifugum. J. Nat. Prod. 1980;43:296–301.

Liang W, Wu X, Fang W, Zao Y, Yang Y, Hu Z, et al. Network meta-analysis of erlotinib, gefitinib, afatinib and icotinib in patients with advanced non-small-cell lung cancer harboring EGFR mutations. PLoS One. 2014;9(2):e85245.

Lipinski CA. Lead- and drug-like compounds: the rule-of-five revolution. Drug discovery today. Technologies. 2004;1(4):337–341.

Martonák R, Laio A, Parrinello M. Predicting crystal structures: the parrinello-rahman method revisited. Phys. Rev. Lett. 2003;90(7):075503.

Matei D, Chang DD, Jeng MH. Imatinib mesylate (Gleevec) inhibits ovarian cancer cell growth through a mechanism dependent on platelet-derived growth factor receptor alpha and Akt inactivation. Clin Cancer Res. 2004;10(2):681–690.

McConkey BJ, Sobolev V, Edelman M. The performance of current methods in ligand-protein docking. Curr Sci. 2002;83(7):845–855.

Morris GM, Huey R, Lindstrom W, Sanner MF,Belew RK, Goodsell DS, et al. AutoDock4 and AutoDockTools4: Automated docking with selective receptor flexibility. J Comput Chem. 2009;30(16):2785–2791.

Mukesh B, Rakesh K. Molecular docking: A review. Int J Res Ayurveda Pharm. 2011;2:1746–1751.

Na Y. Recent cancer drug development with xanthone structures. J Pharm Pharmacol. 2009;61(6):707–712.

Pettersen EF, Goddard TD, Huang CC, Couch GS, Greenblatt DM, Meng EC, et al. UCSF Chimera--a visualization system for exploratory research and analysis. J Comput Chem. 2004;25(13):1605–1612.

Pires DEV, Blundell TL, Ascher DB. pkCSM: Predicting small-molecule pharmacokinetic and toxicity properties using graph-based signatures. J. Med. Chem. 2015;58(9):4066–4072.

Pronk S, Páll S, Schulz R, Larsson P, Bjelmar P, Apostolov R, et al. GROMACS 4.5: a high-throughput and highly parallel open source molecular simulation toolkit. Bioinformatics. 2013;29(7):845–854.

Shah A, Sanghvi K, Sureja D, Seth AK. In-silico drug design and molecular docking studies of some natural products as tyrosine kinase inhibitors. Int J Pharm Res. 2018;10(2):256–260.

Singh P, Bast F. In-silico molecular docking study of natural compounds on wild and mutated epidermal growth factor receptor. Med Chem Res. 2014;23(12):5074–5085.

Sung H, Ferlay J, Siegel RL, Laversanne M, Soerjomataram I, Jemal A, Bray F. Global cancer statistics 2020: GLOBOCAN estimates of incidence and mortality worldwide for 36 cancers in 185 countries. CA Cancer J Clin. 2021;71:209–249.

Verlet L. Computer "experiments" on classical fluids. i. thermodynamical properties of lennard-jones molecules. Phys Rev. 1967;159:98–103.

Vijesh AM, Isloor AM, Telker S, Arulmoli T, Fun HK. Molecular docking studies of some new imidazole derivatives for antimicrobial properties. Arab J Chem. 2013;6(2):197–204.

Wahyuningsih TD, Suma AAT, Astuti E. Synthesis, anticancer activity, and docking study of N-acetyl pyrazolines from veratraldehyde. J Appl Pharm Sci. 2019;9(3):14–20.

Woo S, Jung J, Lee C, Kwon Y, Na Y. Synthesis of new xanthone analogues and their biological activity test cytotoxicity, topoisimerase II inhibition and DNA cross-linking study. Bioorg Med Chem Lett. 2007;17(5):1163–1166.

Woo S, Kang D, Kim J, Lee E, Jahng Y, Kwon Y, Na Y. Synthesis, cytotoxicity and topoisomerase ii inhibition study of new thioxanthone analogues. Bull Korean Chem Soc. 2008;29(2):471-474.

Woo S, Kang D, Nam JM, Lee CS, Ha E, Lee E, Kwon Y, Na Y. Synthesis and pharmacological evaluation of new methyloxiranylmethoxyxanthone analogues. Eur J Med Chem. 2010;45(9):4221–4228.

Yuanita E, Pranowo HD, Mustofa M, Swasono RT, Syahri J, Jumina J. Synthesis characterization and molecular docking of chloro-substituted hydroxyxanthone derivatives. Chem J Mold. 2019;14(1):68–76.

Received for publication on 11th October 2023
Accepted for publication on 22nd January 2024